2018

Vapor Compression System Modelica Library for Aircraft ECS

Nicolas Ablanque
Centre Tecnològic de Transferència de Calor (CTTC), Universitat Politècnica de Catalunya (UPC), nicolas@cttc.upc.edu

Santiago Torras
CTTC UPC, Spain, santiago@cttc.upc.edu

Carles Oliet
Centre Tecnològic de Transferència de Calor (CTTC), Universitat Politècnica de Catalunya (UPC), carles@cttc.upc.edu

Jordi Rovira
quim@cttc.upc.edu

Carles David Pérez-Segarra
Heat and Mass Transfer Technological Center – Polytechnic University of Catalonia, Terrassa (Barcelona), Spain, segarra@cttc.upc.edu

Vapor Compression System Modelica Library for Aircraft ECS

Nicolás ABLANQUE[1]*, Santiago TORRAS[1], Carles OLIET[1], Joaquim RIGOLA[1], Carlos-David PEREZ-SEGARRA[1]

[1]Universitat Politècnica de Catalunya – Barcelona Tech (UPC), Heat and Mass Transfer Technological Center (CTTC), Terrassa, Barcelona, Spain
(+34 937398192, +34 937398920, www.cttc.upc.edu)

* Corresponding Author

ABSTRACT

This work presents a Modelica library aimed to simulate vapor compression systems at both steady and transient conditions. The simulation of these specific systems is particularly challenging from both the phenomena and the numerical resolution point of views. The main goal of the library is to provide, not only accuracy and robustness, but also very low computational time. It is worth mentioning that, although the baseline version of the library is currently operative, its development continues in order to improve or add new features.

Most of the components developed for the library are simulated by means of look-up tables or efficiency curves for the sake of quickness. The main efforts were focused on two critical aspects of the system. On the one hand, heat exchanger models were developed based on a switching moving boundary approach in order to have a relatively high ratio between accuracy and resolution time. This method takes into account the distribution of phases along heat exchangers which is crucial for the accurate simulation of evaporators and condensers. The whole heat exchanger domain is divided in three zones, namely, sub-cooled, superheated and two-phase, and its computational time is lower than distributed models as only one control volume per zone is used. On the other hand, several aspects of the whole cycle resolution were tackled with meticulosity, namely, the management of refrigerant amount, the initialization procedure, the thermostatic control loop, the numerical issues at null mass flow rate, the convergence criteria, and other aspects related to the transient simulation. The results shown in this work are devoted to highlight the numerical robustness of the system and its components together with the low computational time required for simulations.

1. INTRODUCTION

The aeronautical industry is developing new environmental control system architectures, based on the more electrical aircraft (MEA) approach, with the aim of improving the overall performance of aircrafts. The analysis of such architectures is complex as several thermal systems interact between each other. Their design is commonly carried out with the support of numerical simulations. The work presented in this document derives from an on-going project aimed to develop a complete Modelica library to simulate environmental control system architectures within the CleanSky2 European research program.

The cabin cooling on large airplanes has been traditionally achieved from poor-efficiency air cycles; instead, the new architectures include high-efficiency vapor compression cycles devoted to supply additional cooling power when needed. These latter cycles are particularly challenging from both the phenomena and the numerical resolution point of views. The results presented in this work are focused on highlighting the most relevant aspects of the vapor compression system (VCS) library development.

The vapor compression system main components models and cycle resolution approaches were developed based on three critical library requirements: accuracy, robustness, and minimum computational time. Most of the components are modeled based on look-up tables or efficiencies for the sake of prediction accuracy and calculation quickness. The simulation of both the condenser and the evaporator is particularly difficult as the refrigerant phases change throughout the component. At first sight, a distributed-type model should be appropriate as it should guarantee

numerical stability and accuracy, however, the time consumption of such models is too high regarding the project requirements (fast resolution is crucial as the complete environmental control system includes many components and cycles linked to each other). Therefore, a switching moving boundary (SMB) approach where the domain is discretized in only three control volumes has been developed. Although these type of models are more complex to implement, their computational time is considerable low and their accuracy could be comparable to that of the distributed ones when appropriate experimental coefficients are used. Additional difficulties were faced when solving the whole refrigerating cycle. In particular, the need of a robust initialization for a wide range of possible boundary conditions, the need of an additional global refrigerant charge balance, the handling of near-zero mass flow rates, as well as other aspects, were tackled with attention to finally meet the robustness and computational time requirements.

The following sections are devoted to present additional details of the components models and the system numerical resolution aspects. Illustrative results are shown to highlight the numerical stability and low time consumption of models. It is worth mentioning that the work is mainly focused on the numerical point of view as the comprehensive validation of the models has not concluded yet.

2. SYSTEM COMPONENTS

The developed library includes models for the main components of the vapor compression cycle, namely, the compressor, the evaporator, the condenser, and the expansion device. It also includes models for all minor components needed such as the tank, the connection tubes, and the bypass valves.

2.1 Compressor

The compressor model used for this numerical study is of the hermetic reciprocating type and consists of two main elements connected in series (centrifugal type compressors are also being developed within the project). The first element stands for the gas inside the shell where both the mass and the energy balances are calculated with their corresponding transient term:

$$\frac{d\rho_c}{dt}V_c = \dot{m}_{in} - \dot{m}_{comp} \tag{1}$$

$$\frac{d(\rho u)_c}{dt}V_c = \dot{m}_{in}h_{in} - \dot{m}_{comp}h_{out} \tag{2}$$

The second element represents the compressor chamber. This element does not include the dynamic term as its time scale is far smaller than the one for the main thermal and fluid-dynamics of the overall system. The mass flow rate and the compression work are calculated from the volumetric and isentropic efficiencies, respectively.

$$\eta_v = \frac{\dot{m}_{comp}}{\rho V_{sw} N} \tag{3}$$

$$\eta_s = \frac{\dot{W}_s}{\dot{W}_{cp}} \tag{4}$$

The two latter expressions are also expressed as a function of the compression ratio from experimental tests or detailed numerical simulations carried out previously.

2.2 Tank

The tank for the studied system is located between the condenser and the expansion valve. The model handles two-phase flows and assumes complete separation of phases but a shared pressure for the whole volume. The mass and energy conservation equations are expressed as follows:

$$\frac{d\overline{\rho}}{dt}V_t = \dot{m}_{in} - \dot{m}_{out} \tag{6}$$

$$\frac{dH}{dt} = \dot{m}_{in}h_{in} - \dot{m}_{out}h_{out} + V_t\frac{dp}{dt} \tag{7}$$

Where the mean density and total enthalpy are calculated from the liquid volume ratio:

$$\varepsilon = V_L / V \tag{8}$$

$$\overline{\rho} = \varepsilon\rho_L + (1-\varepsilon)\rho_g \tag{9}$$

$$H = V_t(\varepsilon\rho_L h_L + (1-\varepsilon)\rho_g h_g) \tag{10}$$

The outlet enthalpy calculation will depend on the tank geometry and characteristics. A simple approach where the outlet enthalpy is equal to the liquid saturation value has been considered for this study.

2.3 Valves

The valve models used for the vapor compression system are based on lumped parameters used to compute the mass flow rate as a function of the pressure difference. The equation includes a constant flow coefficient but also an effective cross-sectional area which is adjusted from an external control signal.

$$\dot{m} = C_v A_{eff}\sqrt{\rho_{in}\Delta p} \tag{5}$$

2.4 Heat exchangers

Both heat exchangers, the evaporator and the condenser, are made up of three main components: the single-phase secondary flow (which could be either liquid or gas), the refrigerant flow (which circulates throughout the vapor compression system), and the intermediate wall (which is the thermal link between the two flows).

The secondary flow is represented with a unique control volume where the energy and mass conservation principles are applied. The solid wall is characterized with its mass together with a mean temperature value. It either transfers or receives heat from each flow and provides thermal inertia to the whole heat exchanger ensemble. The primary flow – the refrigerant - is calculated based on a switching moving boundary approach as it deals with more complex phenomena. In this case, the energy and mass conservation principles are applied over three different control volumes, namely, single-phase gas, two-phase mixture, and single-phase liquid.

The heat exchanger model is defined from general geometry parameters and fed with look-up tables to predict the values of both pressure drop and heat transfer coefficients. These coefficients are tabulated at different mass velocities and could be subjected to additional correction factor to account for temperature effects. The data to fill up the tables should be obtained from experiments or more precise simulations tools. In both cases the wall temperature should be considered constant as the heat exchanger model has a unique temperature for the solid between the two flows. This latter aspect facilitates the fast resolution of the numerical model but restricts the model adaptability when a significant variation of the solid temperature is required. To overcome this limitation, a global correction factor, calculated from the ratio between the experimental and the calculated heat, has been added to the model. For instance, a heat exchanger with a defined geometry but that operates with two different configurations (e.g. counter-current and parallel-current flow) could be solved with the same look-up tables set for the main coefficients but with different global correction factors.

3. SWITCHING MOVING BOUNDARY

Two main different simulation approaches were considered to simulate the refrigerant flow through heat exchangers: finite-volume (FV) and switching moving boundary (SMB). The former method is easier to implement and provides accurate solutions but requires many control volumes and hence, the computational time is much higher. The latter

method needs just three control volumes but has added numerical complexity not only because a mean void fraction has to be calculated but because volumes have variable lengths and may be activated or deactivated. In the present study the efforts were focused on developing a switching moving boundary approach due the need of low computational time. Besides, Bendapudi *et al*. (2008) and Pangborn *et al*. (2015) stated that there is little difference between the two approaches regarding the accuracy achievable against experimental data.

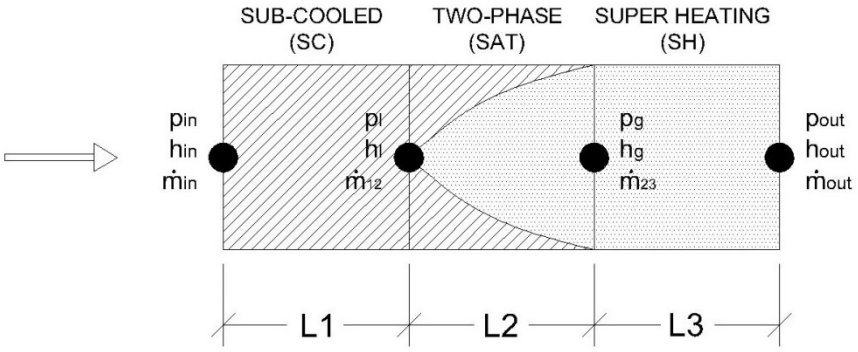

Figure 1: Moving boundary model scheme

The model structure is based on the work presented by Jensen and Tummescheit (2002) where a moving boundary model with a constant number of zones was presented. The flow domain scheme is depicted in Figure 1 and the conservation equations of mass and energy derived for the present model are as follows:

For the sub-cooled zone:

$$A\cdot\left(\rho_{sc}\frac{dL_1}{dt}+L_1\frac{d\rho_{sc}}{dt}-\rho_l\frac{dL_1}{dt}\right)=\dot{m}_{in}-\dot{m}_{12} \tag{11}$$

$$A\cdot\left(\rho_{sc}h_{sc}\frac{dL_1}{dt}+\rho_{sc}\frac{dh_{sc}}{dt}L_1+\frac{d\rho_{sc}}{dt}h_{sc}L_1-L_1\frac{dp_{sc}}{dt}-\rho_l h_l\frac{dL_1}{dt}\right)=\dot{m}_{in}h_{in}-\dot{m}_{12}h_l+Q_{sc} \tag{12}$$

For the two-phase zone:

$$\begin{aligned}A\cdot\left((\bar{\gamma}\rho_g+(1-\bar{\gamma})\rho_l)\frac{dL_2}{dt}+\left(\bar{\gamma}\frac{d\rho_g}{dp}\frac{dp_g}{dt}+(1-\bar{\gamma})\frac{d\rho_l}{dp}\frac{dp_l}{dt}\right)L_2-\rho_g\frac{d(L_1+L_2)}{dt}+\rho_l\frac{dL_1}{dt}+L_2\frac{d\bar{\gamma}}{dt}(\rho_g-\rho_l)\right)\\=\dot{m}_{12}-\dot{m}_{23}\end{aligned} \tag{13}$$

$$\begin{aligned}&A\cdot\left((\bar{\gamma}\rho_g h_g+(1-\bar{\gamma})\rho_l h_l)\frac{dL_2}{dt}+\left(\bar{\gamma}\frac{d\rho_g}{dp}\frac{dp_g}{dt}h_g+\bar{\gamma}\rho_g\frac{dh_g}{dp}\frac{dp_g}{dt}\right)L_2\right)\\&+A\cdot L_2\left((1-\bar{\gamma})\frac{d\rho_l}{dp}\frac{dp_l}{dt}h_l+(1-\bar{\gamma})\rho_l\frac{dh_l}{dp}\frac{dp_l}{dt}\right)\\&A\cdot\left(-L_2\frac{dp_{sat}}{dt}+\rho_l h_l\frac{dL_1}{dt}-\rho_g h_g\frac{d(L_1+L_2)}{dt}+L_2\frac{d\bar{\gamma}}{dt}(\rho_g h_g-\rho_l h_l)\right)=\dot{m}_{12}h_l-\dot{m}_{23}h_g+Q_{sat}\end{aligned} \tag{14}$$

For the superheated zone:

$$A\cdot\left(\rho_{sh}\frac{dL_3}{dt}+L_3\frac{d\rho_{sh}}{dt}+\rho_g\frac{d(L_1+L_2)}{dt}\right)=\dot{m}_{23}-\dot{m}_{out} \tag{15}$$

$$A\cdot\left(\rho_{sh}h_{sh}\frac{dL_3}{dt}+\rho_{sh}\frac{dh_{sh}}{dt}L_3+\frac{d\rho_{sh}}{dt}h_{sh}L_3-L_3\frac{dp_{sh}}{dt}+\rho_g h_g\frac{d(L_1+L_2)}{dt}\right)=\dot{m}_{23}h_g-\dot{m}_{out}h_{out}+Q_{sh} \tag{16}$$

The present model includes additional features compared to the former model of Jensen and Tummescheit (2002):

- Although the mean void fraction derivative with respect to time is commonly neglected in order to have simplified equations, the present model includes it. Recent studies have shown that the void fraction derivative provides better robustness as the state parameters trends become smoother allowing more accurate predictions for fast transients (Desideri *et al.* 2016).
- The pressure drop throughout the domain is calculated following the approach proposed by Qiao *et al.* (2016) which is based on the assumption that the variation is linear.
- The model can switch between different operating modes so that zones could be activated or deactivated according to the flow conditions (see Figure 2). The mass and energy conservation equations of particular zones may be subjected to modifications on local boundary values for each operating mode. Furthermore, following the approach done by Zhang and Zhang (2006), when a zone is deactivated (i.e. the corresponding fluid state is no longer present) its mass conservation equation reduces into an equality between both the local inlet and outlet mass flow rates, while its energy conservation equation is replaced by the length derivative with respect to time which is set to zero. This procedure is necessary to retain the equation set structure solved by Modelica.
- The switching criteria between modes zones has been carefully addressed following a similar approach to that of Bonilla *et al.* (2015). A zone is deactivated whenever its length becomes smaller than a reference minimum length value, and on the contrary, a zone is activated whenever its local outlet enthalpy crosses any boundary saturation enthalpy value. Figure 2 shows all the possible modes and transitions of an evaporator.

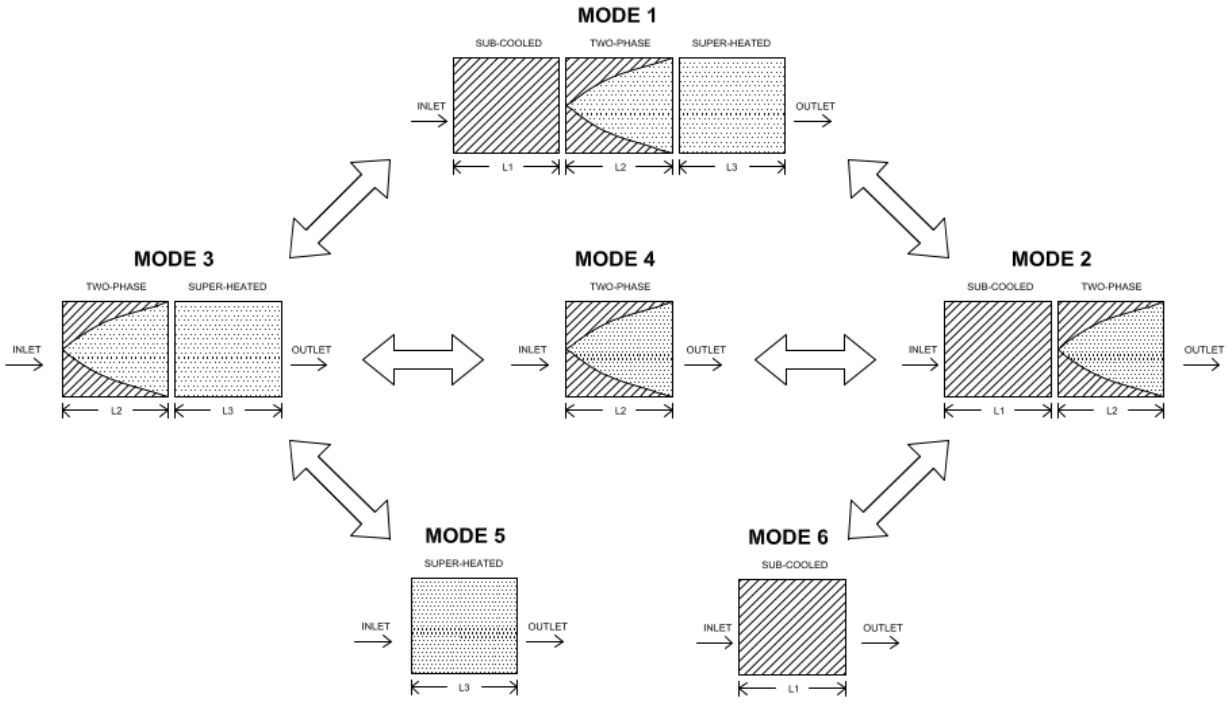

Figure 2: SMB approach: evaporator modes and transitions

The evaporator model has been subjected to a comprehensive set of robustness tests to assess its numerical performance for all transitions between modes. Each transition has been individually and successfully tested by modifying the heat exchanger boundary conditions (i.e. mass flow rates, pressures and inlet specific enthalpies). The switching stability has also been tested: certain inputs were hold constant during simulations while others were varied sinusoidally to force repeated switching. In addition, more demanding tests were conducted by applying variable and asymmetric inlet conditions on both flows. For instance, Figure 3 depicts both the evaporator mode and

zone lengths evolution for independent sinusoidal specific enthalpies inputs on both flows. In this particular case the heat exchanger switches between modes 1, 2, 3 and 4 alternatively as the sub-cooled and the superheated zones are activated or deactivated. The CPU time for this particular case was 1.1 seconds.

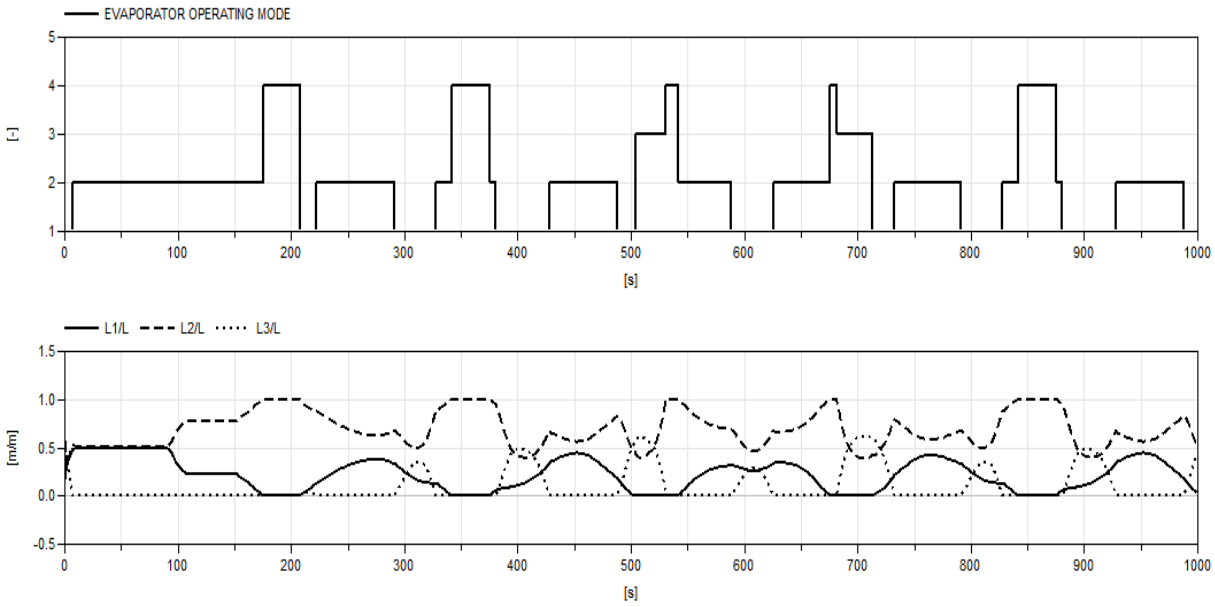

Figure 3: Evaporator transitions robustness test

4. SYSTEM RESOLUTION

The resolution of the closed vapor compression cycle has to face different numerical challenges, namely, the system initialization stability, the strategy to reach a steady-state operating point, the handling of start-up/shutdown events and low/null mass flow rate values, and the management of the system refrigerant charge.

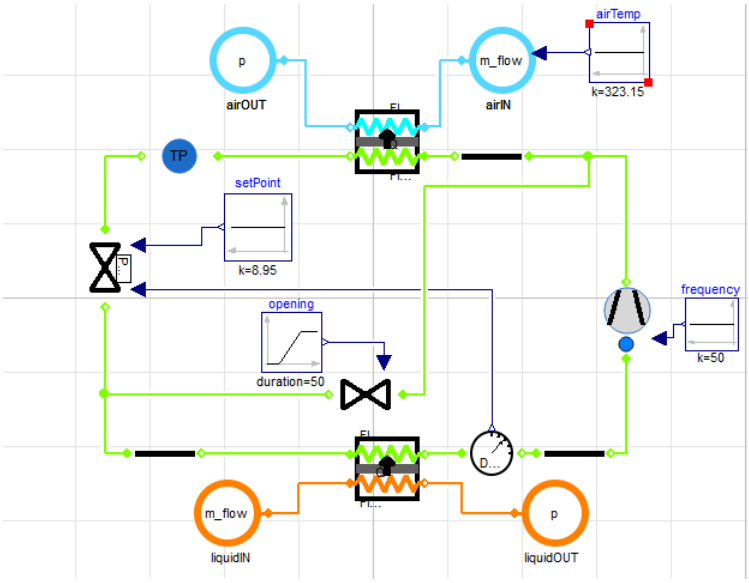

Figure 4: Basic scheme of the studied vapor compression cycle

All of these critical aspects have been tackled in the present work. The layout of the vapor compression system studied herein is shown in Figure 4. The system is made up of a reciprocating compressor, a refrigerant-to-air condenser, a tank enabling refrigerant mass storage or release according to the system thermal needs, a thermo-static valve to control the cycle superheating value at the compressor suction line, a refrigerant-to-water evaporator, and several connecting tubes to calculate local pressure drops. In order to regulate the system operation point, a bypass valve is located between the compressor outlet and the evaporator inlet.

4.1 System steady-state resolution

For the studied VCS, a direct calculation of the initial steady-state cannot be achieved by setting all derivatives equal to zero as it leads to a singularity (the mass flow rate is common to all components and there is no mass exchange at any cycle boundary). Instead, the steady-state is attained by means of an initial meaningless transient relaxation starting from a set of guessed initial values. In the present VCS some components are always solved at steady-state (such as the compressor) but others are solved including the transient terms (such as the accumulator tank). The latter component act as a mass flow buffer and results very helpful for the initialization process, which is a critical issue on closed cycles (Casella, 2012). To facilitate the resolution of components during the initialization, both homotopy transformations and dynamic relaxation of certain variables have been implemented.

The initial values of all the cycle variables are automatically defined from a dedicated global component developed for this task. These values are calculated from two reference temperatures which must be given by the user or, alternatively, taken from the condenser and evaporator secondary flows. Once the simulation is executed, and the initial transient simulation takes place, it finishes when the criteria for the steady-state operating point are fulfilled. These criteria are defined by the user and may include one or more variables from any component of the system.

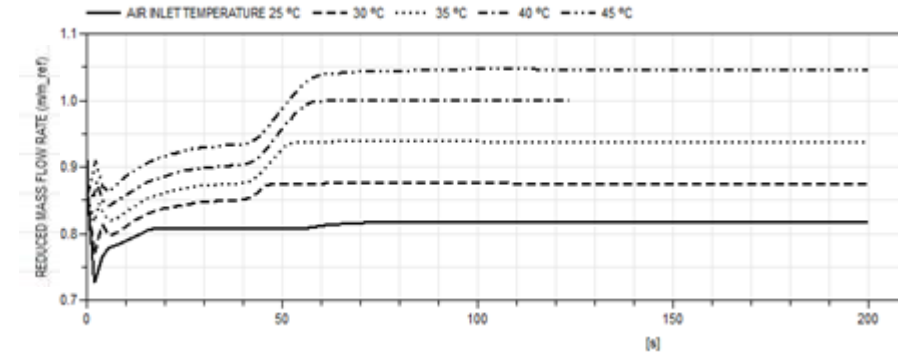

Figure 5: Dimensionless mass flow rate. System steady-state at different inlet air temperatures

A comprehensive set of tests to assess the model initialization and steady-state convergence robustness has been carried out. The system has been simulated considering all possible external parameters, namely, the mass flow rate and temperature of secondary flows in both heat exchangers, the frequency supplied to the compressor, the superheating reference set point value, and the system refrigerant charge. All parameters have been varied over a wide range of values and multiple combinations between them have been considered. For instance, Figure 5 shows the simulation of five cases where the air inlet temperature was changed from 25 to 45 ºC. As observed, all cases attain the steady-state condition after 200 seconds (except for one that converges sooner). The computer time consumption was about 1 second for each case (all the information is given in dimensionless values).

.

4.2 System transient resolution

The system transient response throughout time has also been tested. The results shown in Figure 6 belong to a VCS simulation where the system has been subjected to different externals inputs applied during a unique simulation. First, at time equal to 300 seconds, the compressor frequency is forced to decrease, second, at time equal to 500 seconds, the bypass valve is opened, and third, at time equal to 700 seconds the inlet air temperature is changed. In

this particular case, all changes were obtained from ramp-type signals. The execution time for this specific case was 9 seconds.

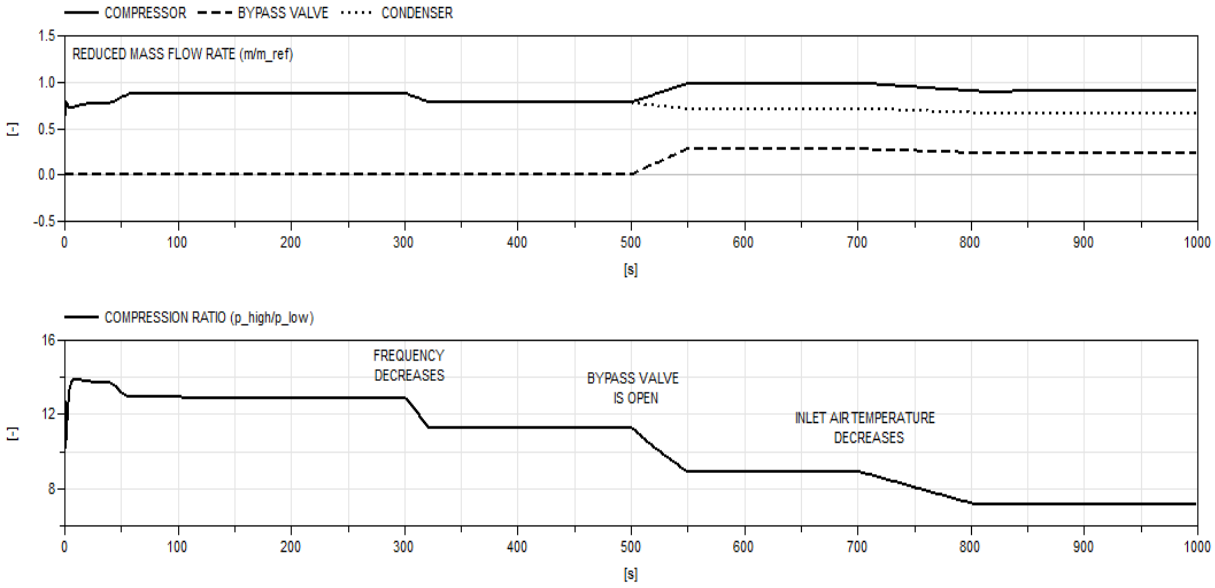

Figure 6: System transient response. Reduced mass flow rate and compression ratio

4.3 System shutdown and start-up

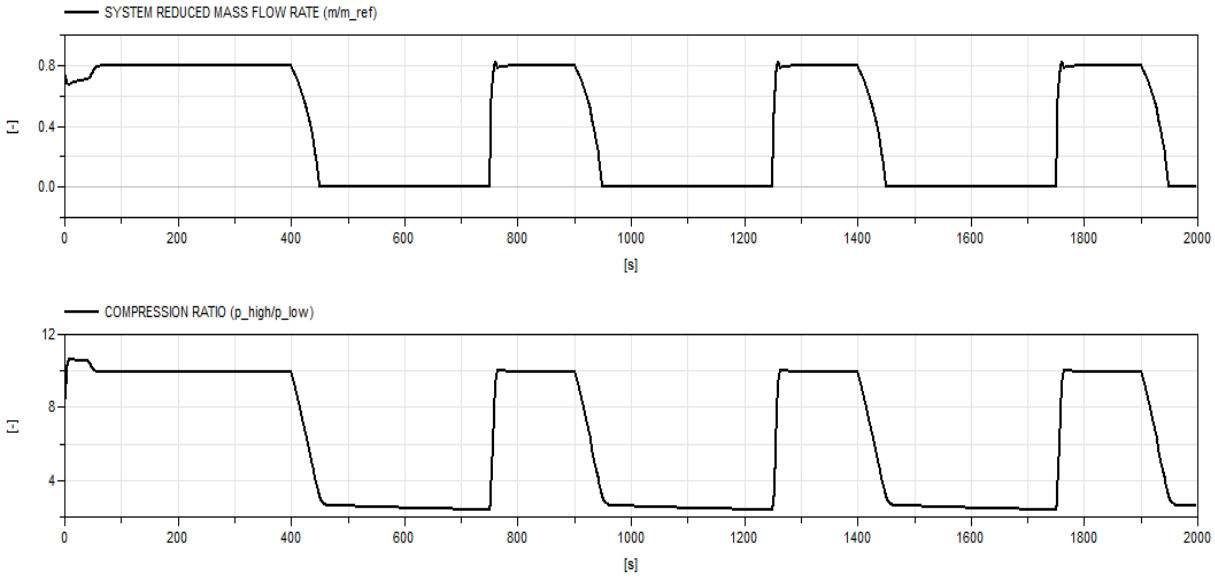

Figure 7: System on/off simulation. Reduced mass flow rate and compression ratio

The resolution of consecutive shutdowns and start-ups is critical for control purposes in some applications. The system simulation at (near) zero mass flow rates is a considerable challenge. At low mass flow rates some oscillations appear due to the fast dynamics in the model so that the solver time step is significantly reduced (Dermont *et al.* 2016). Several numerical aspects should be considered in order to prevent the simulation from failing at such conditions. On the one side, equations must be rearranged to avoid any possible division by zero, and on the other side, regularization should be added to all pressure drop equations. Additional improvements may be

obtained by merging the heat transfer coefficient values of single- and two-phase flows when the mass flow rate approaches zero. Figure 7 shows the evolution when the system is subjected to a cyclic on/off condition.

4.4 Thermo-static valve

The operating point of the vapor compression cycle is controlled by means of a thermo-static valve located between the condenser and the evaporator. This component has two different inputs, namely, the reference superheating value and the actual superheating value (provided by the sensor located at the evaporator outlet). A PID controller with limited output and set point weighting is used to compare the two inputs and to provide an opening degree parameter for the valve (these parameters should be tuned based on experimental data). An illustrative example is shown in Figure 8 where the superheating set point is suddenly increased by 10 ºC.

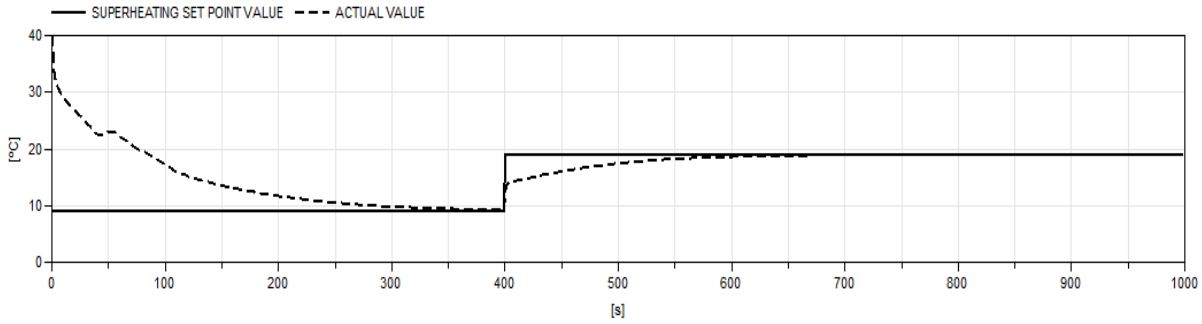

Figure 8: System response to superheating set point value increase

4.5 System refrigerant mass

Another serious aspect to consider is the refrigerant charge management. The total refrigerant amount of the system should somehow be provided during the initialization in order to have a unique solution, otherwise the system will converge to different solutions according to the initial guessed values. Besides, the refrigerant charge amount can experience significant variations during the simulation as long as the mass conservation is not well calculated in all the components. For instance, as stated by Laughman and Qiao (2015), this could happen when two-phase refrigerant flows are present and density values are calculated from enthalpy and pressure (the enthalpy calculation could accumulate small deviations due to the large changes in density when passing from one state to another).

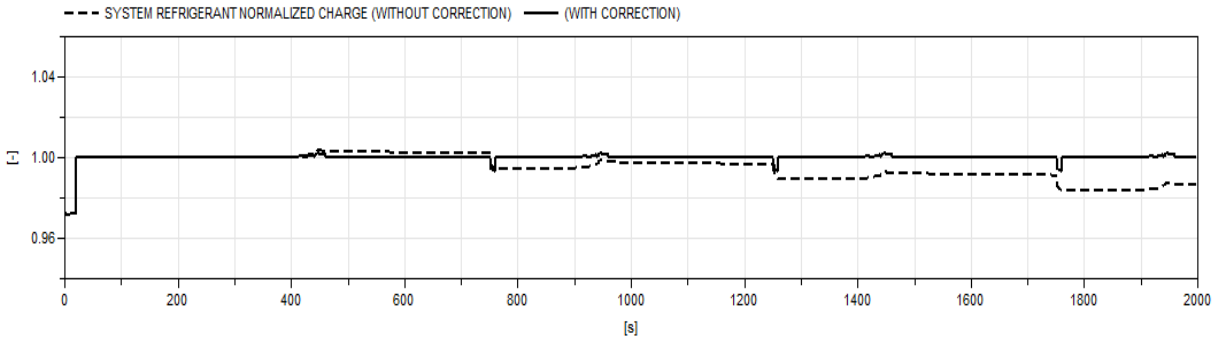

Figure 9: Refrigerant charge conservation. System cyclic on/off simulation

The approach used in the present model consists in correcting the refrigerant system charge whenever its value deviates too much from the reference value. A dedicated global object to manage the refrigerant charge has been developed. The global mass is calculated during every time step and compared to the reference value. Then, if the defined deviation criterion is reached, the component will inject or extract mass artificially to the system. This procedure is done in the tank. Figure 9 shows a comparison of the system when the correction is used and not used.

The results are obtained from the same simulation of Figure 7 as the on/off events generate more drastic changes on components and hence more mass deviations.

5. CONCLUSIONS

A Modelica library to simulate vapor compression systems has been developed and numerically tested. Two main numerical goals were successfully achieved. On the one hand, comprehensive series of tests were carried out to guarantee the system initialization robustness, while on the other hand, the computational time was maintained very low (about one second is needed to run a steady-state operating point). The main efforts were focused on implementing a switching moving boundary model for the heat exchangers and also on tackling with meticulousness the most critical aspects of the closed system resolution. The library development is an ongoing project. The validation of the cycle components is still under process.

NOMENCLATURE

A	cross-sectional area	(m^2)	p	Pressure	(Pa)
h	Specific enthalpy	(J/kg)	Q	heat flow	(W)
H	enthalpy	(J)	U	specific internal energy	(J/kg)
L	length	(m)	V	volume	(m^3)
$\dot{m}$	mass flow rate	(kg/s)	$\dot{W}$	power	(W)
N	frequency	(s^{-1})			
Greek symbols					
ρ	density	(kg/m^3)	γ	void fraction	(-)

REFERENCES

Bendapudi, S., Braun, J. E., & Groll E.A. (2008). A comparison of moving-boundary and finite-volume formulations for transients in centrifugal chillers. *Int. J. Ref., 31*, 1437-1452.

Bonilla, J., Dormido, S., & Cellier, F.E. (2015). Switching moving boundary models for two-phase flow evaporators and condensers. *Comm. Nonlinear Science and Numerical Simulation, 20*, 743-768.

Casella, F. (2012). On the formulation of steady-state initialization problems in object-oriented models of closed thermo-hydraulic system. *Proceedings of the 9th International Modelica Conference, Munich, Germany* (215-222).

Desideri, A., Dechesne, B., Wronski, J., V D Broek, M., Gusev, S., Lemort, V., & Quoilin, S. (2016). comparison of moving boundary and finite-volume heat exchanger models in the Modelica language. *Energies, 9(5),* 339.

Dermont, P., Limperich, D., Windahl, J., Prölss, K., & Kübler, C. (2016). Advances of zero flow simulation of air conditioning systems using Modelica. *Proc. of the 1st Japanese Modelica Conference, Tokyo, Japan* (139-144).

Laughman, C.R., & Qiao, H. (2015). Mass conserving models of vapor compression cycles. *Proc. of the 11th International Modelica Conference, Versailles, France*.

Jensen, J.M., & Tummescheit, H. (2002). Moving boundary models for dynamic simulations of two-phase flows. *In Modelica 2002 Proceedings* (235-244). Modelica Association.

Pangborn, H., Alleyne, A., & Wu, N. (2015). A comparison between finite volume and switched moving boundary approaches for dynamic vapor compression system modeling. *Int. J. Ref.,* 53, 101-114.

Qiao, H., Laughman, C.R., Aute, V., & Radermacher, R. (2016). An advanced switching moving boundary heat exchanger model with pressure drop. *Int. Journal Refrigeration, 65,* 154-171.

Zhang, W. J., & Zhang, C. L., (2006). A generalized moving-boundary model for transient simulation of dry-expansion evaporators under large disturbances. *Int. J. Ref., 29*, 1119-1127.

ACKNOWLEDGEMENT

This work has been developed within the research project “MALET – Development of Modelica Libraries for ECS and Thermal Management Architectures” within the CleanSky2 framework.